Universal relationship between optical emission and absorption of complex systems: An alternative approach

Denise A. Sawicki[1] and Robert S. Knox[1,2]
[1]*Department of Physics and Astronomy, University of Rochester, Rochester, New York 14627-0171*
[2]*Rochester Theory Center for Optical Science and Engineering, University of Rochester, Rochester, New York 14627-0171*
(Received 26 April 1996)

Analyses based on the theories of Kennard and of Stepanov (KS) often claim to support an assumption that emitting manifolds associated with excited electronic states are in thermal equilibrium. KS predict a certain linear $F(\nu)$ with slope $-h/k_BT$, where T is ambient temperature. Variation in $T^*(\nu)=-(h/k_B)/(dF/d\nu)$ reveals the likelihood of extensive excited-state nonequilibration. $T^*(\nu)$, not necessarily an actual temperature, reduces to T under fast relaxation. Its observed variation in certain systems can be modeled with coupled submanifolds far from the equilibrium envisaged by KS. [S1050-2947(96)03912-1]

PACS number(s): 42.50.Md, 33.70.Jg, 32.50.+d, 31.70.Hq

Kennard [1] was probably the first to predict a general relation between the shapes of the absorption and fluorescence spectra of a homogeneous substance. It may be stated in the following form:

$$F(\nu)=\ln\left(\frac{c^2}{8\pi h}\,\frac{I(\nu)}{\nu^3\sigma(\nu)}\right)=-\frac{h\nu}{k_BT}+D(T), \qquad (1)$$

where $I(\nu)$ is the emissive power (W Hz^{-1}) at a particular frequency ν, $\sigma(\nu)$ the absorption cross section at that frequency, k_B Boltzmann's constant, T the ambient temperature, and $D(T)$ a quantity independent of frequency. Stepanov [2] revived interest in the relation in 1957, and it has been widely attributed to him. Others have developed the concept and formulated it for organic molecules, photosynthetic systems, semiconductors, and inhomogeneous systems [3–7]. Its application has generally focused on the goodness of the fit of experimental data to the linear function of frequency suggested by Eq. (1), and the translation of the results into a judgment of how well the excited state has attained thermal equilibrium before emission. In Stepanov's version of the theory, the relation will hold if two conditions are satisfied: first, the aforementioned equilibrium, and second, that ''nonexciting absorption'' (due to transitions between two vibrational levels of the ground state) is negligible. The relation is frequently violated, and we shall see that these two assumptions alone do not give one a sufficiently broad basis to understand the violations.

While Eq. (1) is very general, it is known and applied largely by workers in biofluorescence. We therefore review its derivation. It is a result of applying the Einstein A-B relation to sets of transitions (Fig. 1) in a system characterized by a metastable excited-state population. In the intensity, temperature, and wavelength regimes of interest, stimulated emission is entirely negligible. Thus [2,3]

$$\frac{I(\nu)}{\sigma(\nu)}=\frac{Z\int g'(w')A(w',\nu)p(w')dw'}{Z'\int g(w)B(w,\nu)\exp(-w/k_BT)dw}, \qquad (2)$$

where g and g' are the ground- and excited-state densities of states, respectively, Z and Z' are the partition functions for the ground and excited manifolds, respectively, and A and B are the Einstein coefficients. The important function $p(w')$ is proportional to the probability of occupation of the states at w' and will be central to our subsequent discussion. When the A-B relation is introduced with concern for densities of states,

$$g'(w')A(w',\nu)dw'=\frac{8\pi h\nu^3}{c^2}\,g(w)B(w,\nu)dw, \qquad (3)$$

we obtain

$$\frac{c^2}{8\pi h}\,\frac{I(\nu)}{\nu^3\sigma(\nu)}=\frac{Z\int g(w)B(w,\nu)p(w')dw}{Z'\int g(w)B(w,\nu)\exp(-w/k_BT)dw}. \qquad (4)$$

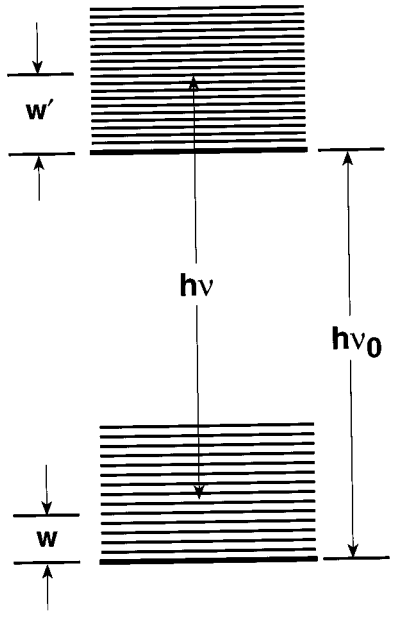

FIG. 1. Relative positions of the energy levels involved in constructing Eq. (5), showing a transition at energy $h\nu$ between two different vibrational sublevels of the ground (w) and excited (w') states.

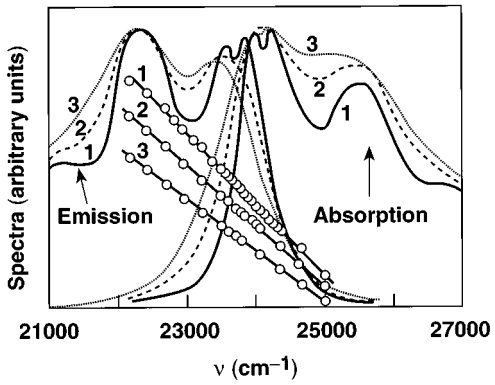

FIG. 2. Absorption and emission spectra of perylene vapor at 513 K (1), 633 K (2), and 713 K (3), and the corresponding Kennard-Stepanov functions (straight lines). Note the correct qualitative temperature dependence of the slope of $F(\nu)$. These straight lines cover over three decades on the vertical scale and yield effective temperatures 556, 655, and 755 K, respectively. After Borisevich and Gruzinskii [8].

At each ν, the states in the vicinity of w' are connected to specific groups of states in the vicinity of w in the lower manifold and their energies are related by

$$h\nu_0 + w' = h\nu + w. \tag{5}$$

Therefore

$$\frac{c^2}{8\pi h}\,\frac{I(\nu)}{\nu^3\sigma(\nu)} = \frac{Z\int g(w)B(w,\nu)p(w+h\nu-h\nu_0)dw}{Z'\int g(w)B(w,\nu)\exp(-w/k_BT)dw}. \tag{6}$$

Equation (6) is still quite general, and, when p is replaced by the Boltzmann distribution and $h\nu_0$ is set equal to zero, it reduces to the Wien law at photon frequencies of interest to us. What distinguishes the fluorescent case from the blackbody case is that the fluorescence has an artificially induced metastable population based on the energy $h\nu_0$ (such as, for example, the 0-0 electronic energy separation in a complex molecule). Kennard and Stepanov assumed such a metastable situation in a fluorescent system and made the further key assumption that the excited system was thermally equilibrated:

$$p(w') = \exp(-w'/k_BT) = \exp[-(w+h\nu-h\nu_0)/k_BT]. \tag{7}$$

Introduction of this distribution into (6) leads immediately to Eq. (1), and tells us that the quantity $D(T)$ is the system-specific quantity $h\nu_0/k_BT + \ln(Z/Z')$. The careful identification of $D(T)$ is due to Neporent [3].

Ordinarily, the relation (1) is checked for a substance by finding the slope of $F(\nu)$ from experimental data and comparing T, as determined from this slope, with the ambient temperature. The most reliable data are those from the Stokes region, where both absorption and emission are at a high fraction of their maximum values. Experimenters have almost always found the relationship to be ''half right''—the function $F(\nu)$ is a reasonably straight line over much of the Stokes region, but, remarkably, the deduced value of T has seldom agreed with the ambient temperature (see, e.g., Fig. 2, taken from Borisevich and Gruzynskii [8]). For this reason, one adopts the notation T^* for the effective temperature deduced from the slopes. In some experiments, T^* has been considerably higher than ambient temperature and in a few cases it has been lower. There has been much speculation as to the causes of these particular deviations from the relation. Many cases are reviewed and discussed by Van Metter and Knox [6], who evaluated inhomogeneous broadening as a possible cause.

The observed linear function that remarkably arises from very complex input is a broad confirmation of the ''universal relation,'' but its failure in detail is symptomatic of the possibility of a very complex nonequilibrium distribution during the lifetime of the fluorescence. The experiments yielding $T^* \neq T$ seem to tell us that this distribution is nearly equilibrated, although the conclusion that the excited molecule has a ''warm'' environment is inconsistent with a single temperature appearing in the theory [6]. Here we report a method of analyzing the Kennard-Stepanov (KS) data that highlights the deviation from a Boltzmann distribution. We find that the failure of the slope to produce an ambient temperature value is only one aspect of this deviation, and we set forth a phenomenological theory on the basis of which some of the observations can be understood.

The Kennard-Stepanov *spectral temperature* is defined in terms of the local slope of $F(\nu)$:

$$T^*(\nu) \equiv -\left[\frac{k_B}{h}\,\frac{d}{d\nu}\ln\left(\frac{c^2}{8\pi h}\,\frac{I(\nu)}{\nu^3\sigma(\nu)}\right)\right]^{-1}. \tag{8}$$

This device transforms the rather prosaic experimental $F(\nu)$ into a spectrum which, in most cases seen to date, is rich in detail. There are peaks, valleys, plateaus, and sometimes divergences. In virtually no case to date have we found a constant $T^*(\nu)$, as the KS relation predicts. $T^*(\nu)$ curves computed from data sets [9–12] in several typical cases are shown in Fig. 3. A frequently seen feature is that $T^*(\nu)$ remains fairly constant either near ambient temperature or somewhat above it over much of the frequency range, but includes one or more peaks.

In practice, $T^*(\nu)$ is found from the inverse slope of the regression line through $F(\nu)$ for a series of data points centered at frequency ν. The width of the derivative window can be varied. A larger window is necessary when there seems to be a great deal of experimental noise. In most cases, the slope has been best found over a number of data points ranging between 5 and 11. Generally, changing the width of the derivative window has only a very slight effect upon the contour of $T^*(\nu)$. By introducing artificial noise and artificial miscalibrations into simulated data, we have satisfied ourselves that the structures seen are not artifacts of the method. Also, the effects appear to be reproducible, as discussed below.

Before discussing the possible origins of the structure appearing in Fig. 3, we describe the materials on which it is based. We have found it difficult to rely on the published literature for the accuracy necessary in this study, so in most cases unpublished data in electronic form have been used. Figures 3(a) and 3(b) refer to solutions of a subunit of an important photosynthetic antenna protein, α-phycocyanin (α-

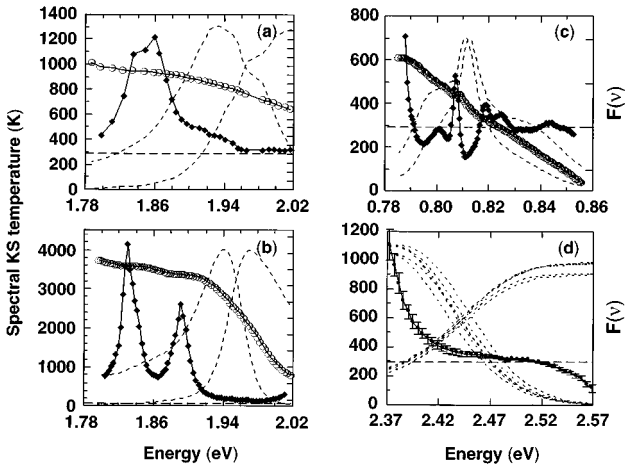

FIG. 3. Experimental $T^*(\nu)$ spectra (filled diamonds) and the parent $F(\nu)$ (open circles). Dashed curves in the background are emission (on the left) and absorption (on the right). Spectra are in arbitrary units, $T^*(\nu)$ is in K, and the variation of $F(\nu)$ is indicated by tick marks, separated by factors of 2.303, at the right of each frame except (d). The abscissa is frequency in energy units. (a) α-phycocyanin, 295 K (Sauer [9]); (b) α-phycocyanin, 77 K (Debreczeny *et al.* [10]); (c) erbium-doped silicate glass, 295 K (Giles and DeSurvire [11]); (d) poly (p-phenylene vinylene) [12]. In each case the constant value of the ambient temperature, which is the prediction of the universal relation for T^*, is shown as a horizontal dashed line. In (d) the spectral temperature computed from six absorption-emission pairs is shown as a mean with standard deviation indicated by error bars. Here $F(\nu)$ is not shown, for clarity.

PC). Figure 3(a) shows one of the first cases we analyzed. Sauer [9], who brought its unusual KS behavior to our attention several years ago, computed $F(\nu)$ from room-temperature fluorescence and absorption spectra of α-PC representative of samples from four different organisms (Switalski and Sauer [13]). The four α-PC had similar fluorescence, absorption, and circular dichroism spectra, similar time-resolved fluorescence behavior, and high fluorescence polarization across the entire band of excitation wavelengths. Care was taken to test for the presence of α-β heterodimers.

The data from which Fig. 3(b) was produced were those of Debreczeny and colleagues [10]. Again the system is the subunit α-PC, this time at 77 K in a buffer of 5 mM phosphate at pH 7.0 with 75% glycerol by volume. The small rise near 2.02 eV should be ignored as it may be a result of scattering from the 560-nm excitation source.

Figures 3(c) and 3(d) show KS analyses for two materials of interest to applied physics. The former represents room-temperature Er-doped silicate glass codoped with Al and Ge [11], one of the important materials for use in fiber light amplifiers. The latter shows spectral temperatures computed from the spectra of a series of poly(p-phenylene vinylene) (PPV) samples [12], materials of interest for use in light emitting diodes. The several PPV cases shown represent data from samples subjected to different periods of aging; these will be discussed below as an example of reproducibility of the curves. The case of Fig. 3(c) illustrates the remarkable amount of structure that sometimes presents itself as a KS spectral temperature.

The existence of peaks in certain $T^*(\nu)$ data may be understood physically on the basis of the following straightforward model. A system of fluorescing states is considered as a mixture of individual systems within each of which there is thermal equilibration and among which detailed-balance kinetics with adjustable rates can be applied. This is a natural development of an idea introduced by Band and Heller [7]. In terms more closely related to our context, each subsystem of fluorescers is a ''KS system'' that contributes absorption and fluorescence components obeying Eq. (1) but whose populations relative to each other are kinetics dependent. The subsystems may in fact be chemically different molecules or sets of chemically identical molecules which are inhomogeneously broadened or they may represent manifolds associated with different electronic states of each molecule of a homogeneous species.

It is readily shown that the KS function for the KS mixture just described is given by

$$F(\nu)=\ln\left(\sum_i \overline{p_i}\xi_i(\nu)\exp[F_i(\nu)]\right), \tag{9a}$$

where $\overline{p_i}$ is the average relative population of the emitting subset i, $F_i(\nu)$ is the KS function for that subset, and

$$\xi_i(\nu)=\frac{\sigma_i(\nu)}{\Sigma_j\sigma_j(\nu)}. \tag{9b}$$

From this, we can discern that, for a system in which the absorption and emission spectra are linear combinations of the individual spectra of n species each of which obey Eq. (1), $F(\nu)$ will have n asymptotes of slope $-h/k_BT$. In a mixture of two species that do not exchange excitation energy (noninteracting species), the spacing between the intercepts will be equal to the difference between the two values of $D(T)$.

The addition of excitation exchange between the manifolds makes the situation slightly more complex. We solve the kinetic equations for the steady-state manifold populations $\overline{p_i}$, assuming that the exciting light comes at a constant rate and using transfer rates, intrinsic quantum yields, relative oscillator strengths, and spectral shape functions as inputs. The choice of a model Gaussian absorption peak combined with the KS function and the values of Z and Z' dictates the model emission peak of a manifold. In Fig. 4 we show the effect of varying two of the parameters relating two coupled manifolds whose associated absorption peaks are Gaussians centered at 1.85 and 1.90 eV [each with full width at half maximum (FWHM) 0.10 eV]. For simplicity all partition functions are assumed equal. From top to bottom the ratio of oscillator strengths is varied, with values 5:1, 1:1, and 1:5 [(1.85-eV band):(1.90-eV band)]. From left to right the intermanifold rate constant k for 1.90-to-1.85 transfer is varied, taking values 0, 1, and 10 in units of the larger fluorescence rate of the pair. The corresponding upward transfer rates are modified by the Boltzmann factor, $\exp(-\Delta E/k_BT)=0.145$ at 300 K. As noted above, since the manifolds correspond to ''good KS systems,'' the two emission bands are automatically determined. Their peak positions occur at 1.78 and 1.83 eV, respectively. We assume broadband excitation and an intrinsic quantum yield of 1.0 for each. In all parts of Fig. 4 the absorption and emission

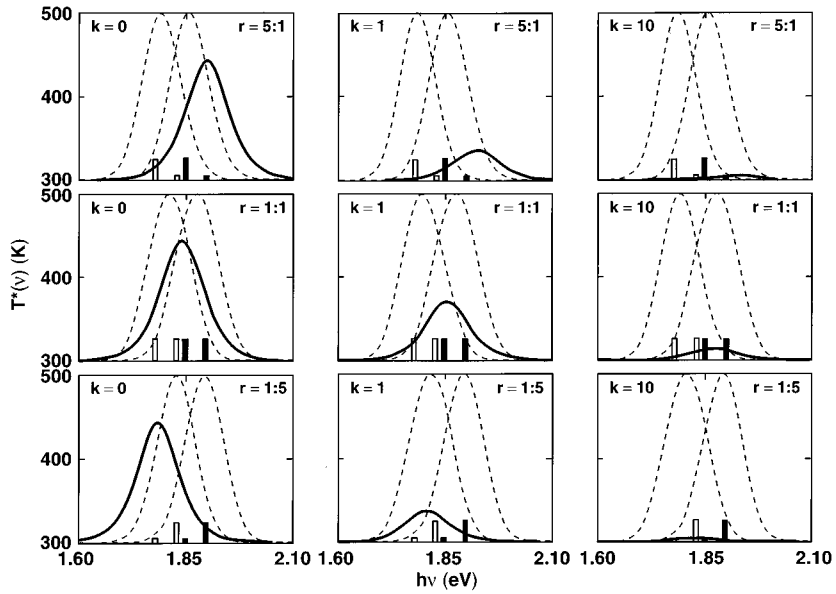

FIG. 4. Results of model calculations of $T^*(\nu)$, with manifolds as described in the text. Parameters: r is the ratio of the oscillator strength of a Gaussian absorption band, FWHM 0.010 eV, centered at 1.85 eV to that of a similar band centered at 1.90 eV. Small bars indicate the locations and relative strengths of the absorption bands (filled bars) and emission bands (open bars). The total absorption and emission are shown as dashed lines, adjusted to full scale. k is the downward transfer rate (from the 1.90 manifold to the 1.85 manifold) in units of the larger of the two fluorescence rates. Because quantum yields are taken to be unity and broadband excitation is assumed, these two parameters, along with the Boltzmann factor that determines the upward transfer rate of $0.145k$, define the kinetic system completely.

envelopes, scaled to equal height, are shown in the background. The underlying manifolds are not resolved.

Reading Fig. 4 left to right, one sees the approach to excited-state equilibrium conditions. $T^*(\nu)$ approaches its constant value 300 K as k increases. This figure also shows that for the (typical) spectral parameters chosen, appreciable structure exists in $T^*(\nu)$ only when k drops below about ten times the fluorescence rate; this is rather slow in terms of normally assumed intramolecular relaxation rates. Also illustrated is the dependence of the $T^*(\nu)$ peak position on the oscillator strength ratio. At equal oscillator strengths and zero transfer, the peak is at the midpoint of the Stokes region. As the oscillator strength ratio becomes farther from unity, the peak follows the weaker band. These characteristics remain, in slightly moderated form, as the transfer rate increases.

More generally, there will be at most $n-1$ peaks in $T^*(\nu)$ for n excited manifolds. These peaks correspond to the visibly nonlinear portions between the asymptotes of $F(\nu)$. When $F(\nu)$ includes one or more segments of positive slope, $T^*(\nu)$ will be undefined where the slope momentarily crosses zero, and may become negative. The number of species present is not necessarily evident from looking at a plot of $T^*(\nu)$, because some of the peaks may be small enough that they would be indistinguishable from experimental noise or two or more peaks may be so close together that they resemble one.

The full modeling of spectra must account also for $T^*(\nu)$ dropping below ambient, in some cases becoming divergent. Our exploration of parameter space has shown that dips below ambient are indicative of the higher-energy species having a low quantum yield, and that divergences occur when there is broadband excitation of weakly coupled manifolds whose separation is greater than their widths. Variation in the curves with excitation wavelength is readily treated with the kinetic model, in analogy with the variation of the standard T^*, discussed and reviewed by Van Metter and Knox [6]. Variation of the standard T^* was observed in splendid detail recently by Sechkarev and Beger [14] in adsorbed rhodamine 6G, a system for which the present analysis should provide an even richer basis for analysis of the relaxation.

The systems of Fig. 3 are complex, and we have had only limited success in fitting the curves using this elementary relaxation model. The α-PC peaks in Figs. 3(a) and 3(b) are sufficiently stable and reproducible that the existence of poorly coupled states, as in our model, is a good possibility. Should they represent impurities, it is clear that the KS analysis is a sensitive method for locating them. The T^* variations in Figs. 3(c) and 3(d) may well be indicative of single-manifold KS failure. Another consideration is inhomogeneous broadening [6], which, in a case involving a single species, causes an upward shift in the value of the ordinary T^* and, if the excitation is not broadband, introduces some weak ν dependence into $T^*(\nu)$. Adding inhomogeneous broadening into the computer simulation might make it possible to model a case resembling the 77-K data of Debreczeny *et al.* [10], Fig. 3(b), in which the contour of the $T^*(\nu)$ plot resembles the theoretical case of a mixture of species, but in which $T^*(\nu)$ never goes as low as ambient temperature.

It is necessary to address the question of reproducibility of the experimental effects. Of course this is primarily a matter of reproducibility of the spectra involved, but $T^*(\nu)$ senses small relative changes, in analogy with derivative spectroscopy. In the case of α-phycocyanin, Debreczeny's 295-K data (not shown) are very similar to Sauer's [Fig. 3(a)], a main peak occurring at 1.87 eV and an additional one

outside Sauer's range at 1.80 eV. As the temperature is lowered, these peaks apparently shift and interchange strengths, ending up at 1.89 and 1.83 eV at 77 K [Fig. 3(b)]. The data on PPV, Fig. 3(d), provide a good example of $T^*(\nu)$ reproducibility. The several dashed curves shown are absorption and emission spectra of six different samples. While in this case the data come from the same laboratory [12], each sample was grown from a different precursor aged for six separate periods of time. When judging reproducibility, we must recognize that the utility of the $T^*(\nu)$ analysis brings with it the cost of high sensitivity to those experimental conditions that affect equilibrium among various manifolds of states.

In summary, we have shown the usefulness of plotting a function $T^*(\nu)$ in order to magnify regions of nonlinearity in the KS function. Experimenters have often disregarded the nonlinearity of these plots. As we have seen, however, peaks in $T^*(\nu)$ could be sensitive indicators of the presence of hidden excited states or impurities with which there is incomplete thermal equilibration. $T^*(\nu)$ should prove useful as a means of estimating transfer rates in complex molecules where the participating states are already identified. We are persuaded by the data and by results such as those of Fig. 4 that our interpretation is correct, and that efforts to examine the full parameter space will be rewarded.

We thank Kenneth Sauer for supplying the unpublished data of Fig. 3(a) and for stimulating correspondence. Martin Debreczeny and C. Randy Giles kindly supplied the published data of Figs. 3(b) and 3(c), respectively, in electronic format. Matt Robinson and Yongli Gao kindly provided a prepublication copy of Ref. [12] and the data of Fig. 3(d). We acknowledge the lively discussions with Philip Laible and Thomas Owens that helped launch this project. The research was sponsored in part by the U.S. Department of Agriculture, NRI Competitive Grants Office Project No. 95-37306-2014 and in part by the National Science Foundation under Grants No. 94-00059 and No. 94-15583.

[1] E. H. Kennard, Phys. Rev. **11**, 29 (1918); **28**, 672 (1926).
[2] B. I. Stepanov, Dokl. Akad. Nauk SSSR **112**, 839 (1957) [Sov. Phys. Dokl. **2**, 81 (1957)].
[3] B. S. Neporent, Dokl. Akad. Nauk SSSR **119**, 682 (1958) [Sov. Phys. Dokl. **3**, 337 (1958)].
[4] R. T. Ross, Photochem. Photobiol. **21**, 401 (1975).
[5] D. E. McCumber, Phys. Rev. **136**, A954 (1964).
[6] R. L. Van Metter and R. S. Knox, Chem. Phys. **12**, 333 (1976).
[7] Y. B. Band and D. F. Heller, Phys. Rev. A **38**, 1885 (1988).
[8] N. A. Borisevich and V. V. Gruzinskii, Opt. Spektrosk. **14**, 39 (1963) [Opt. Spectrosc. (USSR) **14**, 20 (1963)].
[9] K. Sauer (unpublished data).
[10] M. P. Debreczeny, K. Sauer, J. H. Zhou, and D. A. Bryant, J. Phys. Chem. **97**, 9852 (1993); **99**, 8412 (1995).
[11] C. R. Giles and E. DeSurvire, J. Lightwave Technol. **9**, 271 (1991).
[12] M. R. Robinson, H. Rasafitrimo, Y. Gao, and B. R. Hsieh, Polym. Mater. Sci. Eng. **74**, 292 (1996).
[13] S. C. Switalski and K. Sauer, Photochem. Photobiol. **40**, 423 (1984); S. C. Switalski, Ph. D. thesis, University of California Berkeley, 1986.
[14] A. V. Sechkarev and V. N. Beger, Opt. Spektrosk. **72**, 560 (1992) [Opt. Spectrosc. (USSR) **72**, 303 (1992)].